Supporting Information

Out-plane Fe^{II}-N_4 moiety modified Fe-N co-doped porous carbons as high-performance electrocatalysts for oxygen reduction reaction

Zhongjie Qian, Zhaowen Hu, Zhengping Zhang, Zhilin Li, Meiling Dou*, Feng Wang*

State Key Laboratory of Chemical Resource Engineering, Beijing Key Laboratory of Electrochemical Process and Technology for Materials, Beijing University of Chemical Technology, Beijing 100029, P R China

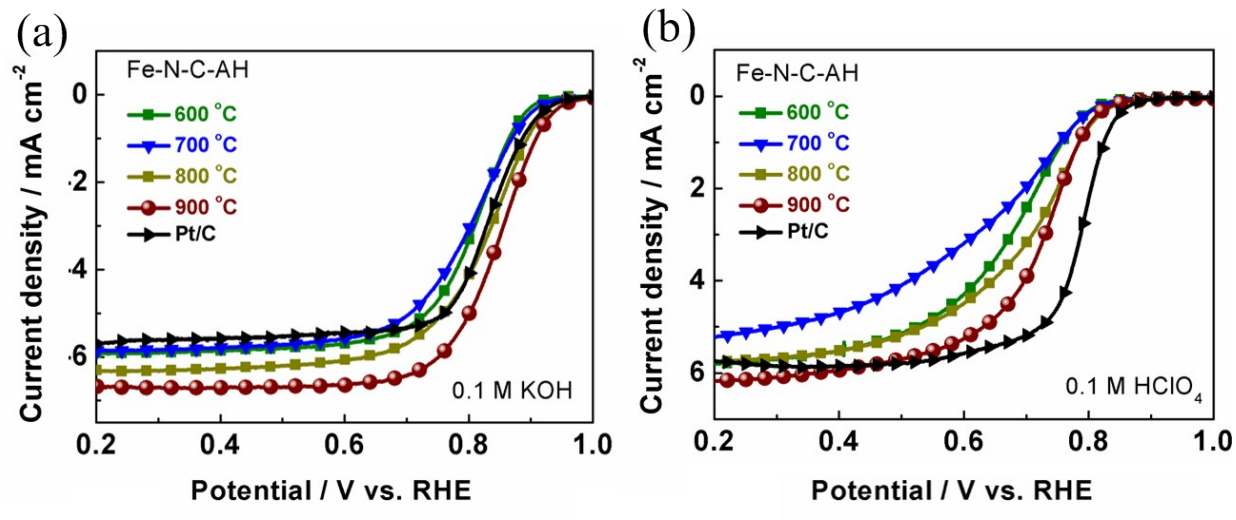

Fig. S1. LSV curves of Fe-N-C-AH electrocatalysts prepared with various pyrolysis and post-treatment temperatures profiled in O_2-saturated (a) 0.1 M KOH and (b) 0.1 M $HClO_4$ (scan rate: 5 mV s^{-1}, electrode rotation rate: 1600 rpm).

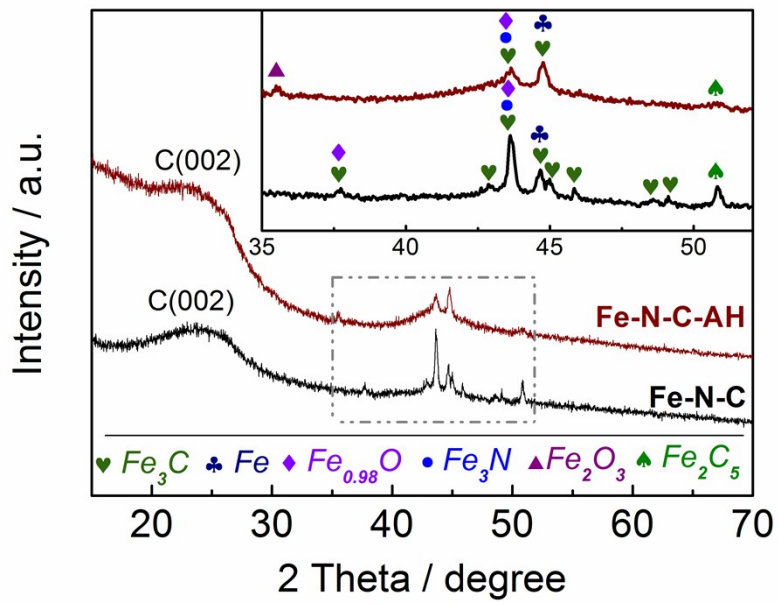

Fig. S2. XRD patterns of Fe-N-C and Fe-N-C-AH.

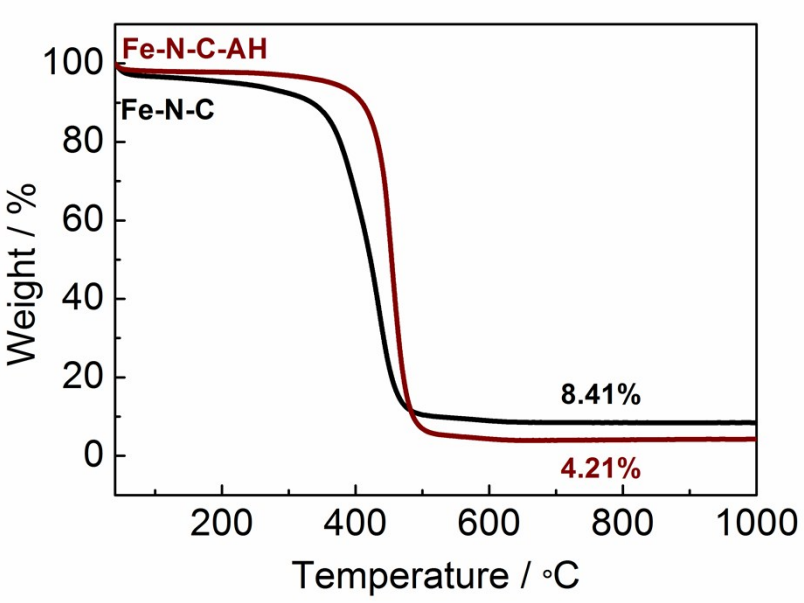

Fig. S3. TG profiles of Fe-N-C and Fe-N-C-AH.

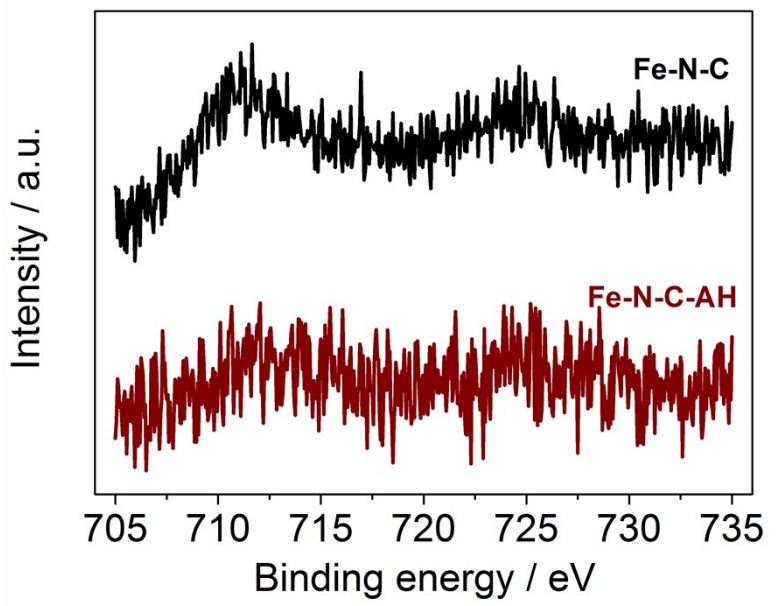

Fig. S4. Fe *2p* XPS spectra of Fe-N-C and Fe-N-C-AH.

Table S1. Pore characteristics of Fe-N-C and Fe-N-C-AH.

Sample	S_{BET} (m^2 g^{-1})	S_{micro} (m^2 g^{-1})	S_{micro} / S_{BET} (%)	V_{pore} (cm^3 g^{-1})	V_{micro} (cm^3 g^{-1})	V_{micro} / V_{pore} (%)
Fe-N-C	425.4	161.2	37.89	0.5454	0.069	12.65
Fe-N-C-AH	711.1	423.7	59.58	0.7289	0.182	24.96

Table S2. The content and configuration of N for Fe-N-C and Fe-N-C-AH.

Sample	N at. %	Relative content of different N species				
		Pyridinic N	Fe-N_4	Pyrrolic N	Graphitic N	Oxidized N
Fe-N-C	2.21	32.30	22.15	25.55	10.92	9.08
Fe-N-C-AH	1.91	24.86	18.47	23.30	25.82	7.55

Table S3. Summary of the Mössbauer parameters for Fe-N-C and Fe-N-C-AH.

MS site	δ_{iso}[a] / mm s^{-1}	ΔE_Q[b]	Fwhm[c] / mm s^{-1}	H_0[d] / T	Assignment
Sing	-0.05		0.43		Superparamagnetic iron
D1	0.31	0.983	0.58		Fe^{II}-N_4/C, low-spin
D2	0.21	1.19	0.58		Fe^{II}-N_4, mid-spin
Sext	0.17	-0.003	0.45	20.9	Iron carbide

[a]δ_{iso}: the isomer shift that related to the electric monopole interaction; [b]ΔE_Q: the quadrupole splitting that related to the electric quadrupole interaction; [c]Fwhm: the full-width at half maximum; [d]H_0: the magnetic field.